

typical nuclear dimensions³ (see Fig. 3.1.3). In a two-nucleon transfer process this virtual property becomes real, in the sense that the presence of (normal) density over regions larger than that of the dimensions of each of the interacting nuclei allows for incipient ξ nuclear Cooper pair manifestation.

Within this context, let us refer to the Josephson effect, associated with the Cooper pair tunneling across a thin barrier separating two metallic superconductors. Because the probability of one-electron-tunneling is of the order of 10^{-10} , (conventional) simultaneous tunneling associated with a probability of $(10^{-10})^2$ would hardly be observed (cf. Sect 3.3). Nonetheless, Josephson currents are standard measures in low temperature laboratories⁴.

The same arguments related to the large value of the correlation length is operative in explaining the fact that Coulomb repulsion is rather weak between partners of Cooper pairs which are, in average, at a distance $\xi (\approx 10^4 \text{ \AA})$ much larger than the Wigner–Seitz radius r_s typical of metallic elements ($\approx 1 - 2 \text{ \AA}$). Consequently, it can be overwhelmed by the long range electron–phonon pairing. Similarly, in widely extended light halo nuclei, the short range bare pairing interaction plays little role, becoming subcritical (cf. Sect. 2.6). The fact that such systems are nonetheless bound, although weakly, testifies to the dominant role the exchange of collective vibrations between halo nucleons have in binding the associated halo Cooper pair (e.g. $^{11}\text{Li(gs)}$, and, arguably, also⁵ of ^{12}Be (0^{++} ; 2.251 MeV) to the core ($^9\text{Li(gs)}$ and ^{10}Be respectively) (cf. Section 6.1.2).

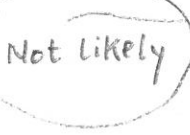
The above arguments are at the basis of the fact that second order DWBA theory which add both successive and non-orthogonality contributions to the simultaneous transfer amplitudes, provides a quantitative account of the experimental findings (see e.g. Figs. 2.1.6, 3.4.2 (a), 3.4.3 (a) and Chapter 6).

3.2 Two-nucleon transfer probabilities

As discussed in Chapter 1, the enhancement factor in a two-nucleon transfer reaction can be defined in terms of two-particle units⁶, similar to what is done in the case of electromagnetic decay (Weisskopf units)⁷. Let us, for simplicity, write such a relation as

$$\frac{d\sigma}{d\Omega} \Big|_{2n} = |\langle f | P^\dagger | i \rangle|^2 \left(\frac{d\sigma}{d\Omega} \right)^{(0)}_{2n}, \quad (3.2.1)$$

where $\left(\frac{d\sigma}{d\Omega} \right)^{(0)}_{2n}$ is the absolute differential cross section associated with a typical pure single-pair configuration $|j^2(0)\rangle$ (or the average value over pairs based on the

³Within this context one can put the following question. Is anybody worried that a photon can, in a two slit experiment, be broken in two?  Why should then one worry that successive transfer can break a Cooper pair?

⁴cf. e.g. Rogalla and Kes (2012) and references therein.

⁵See e.g. Johansen et al. (2013).

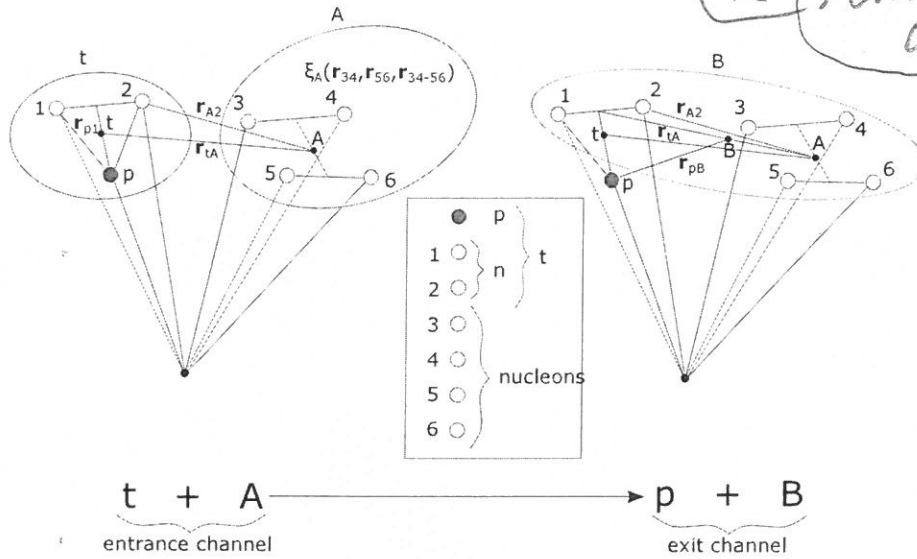
⁶cf. e.g. Broglia, R. A. et al. (1972); Broglia, R.A. et al. (1973) and references therein.

⁷See e.g. Bohr and Mottelson (1969).

figura a la izquierda see scanning original figures, bold face vectors
 figura a la derecha $\vec{t} \cdot \vec{2}$, $\vec{CM(1-2)} - \vec{P}$, $\vec{A} - \vec{t}$, $\vec{2-A}$, $\vec{6-5}$, $\vec{CM(6-5)} - \vec{CM(3-4)}$, $\vec{(4-3)}$
 $\vec{(2-1)}$, $\vec{t-A}$, $\vec{B-P}$, $\vec{3-4}$, $\vec{5-6}$, $\vec{CM(3-4)} - \vec{CM(5-6)}$.

3.2. TRANSFER PROBABILITIES, ENHANCEMENT FACTOR

219



(R) Legend scanning
Original Figures

$$\frac{d\sigma}{d\Omega} = \frac{\mu_i \mu_f}{(2\pi\hbar^2)^2} \frac{k_f}{k_i} \left| T^{(1)} + T_{succ}^{(2)} - T_{NO}^{(1)} \right|^2$$

$$\phi_i(\mathbf{r}_{p1}, \sigma_1, \mathbf{r}_{p2}, \sigma_2) \chi_{m_i}^{1/2}(\sigma_p) \psi_A(\xi_A) \chi_{IA}^{(+)}(\mathbf{r}_{IA}) \quad \chi_{m_i}^{1/2}(\sigma_p) \psi_B(\xi_B) \chi_{PB}^{(-)}(\mathbf{r}_{PB})$$

e.g., in Eq. (5.1.4) $(\phi_d(\mathbf{r}_{p1}, \sigma_1) \phi_d(\mathbf{r}_{p2}, \sigma_2) \chi_{IA}^{(+)}(\mathbf{r}_{IA}))$

$$\Psi_{A+2}(\xi_A, \mathbf{r}_{A1}, \sigma_1, \mathbf{r}_{A2}, \sigma_2) = \psi_A(\xi_A) \sum_{l_i, j_i} [\phi_{l_i, j_i}^{A+2}(\mathbf{r}_{A1}, \sigma_1, \mathbf{r}_{A2}, \sigma_2)]_0^0 \\ = \psi_A(\xi_A) \sum_{nm} a_{nm} [\varphi_{n, l_i, j_i}^{A+2}(\mathbf{r}_{A1}, \sigma_1) \varphi_{m, l_i, j_i}^{A+2}(\mathbf{r}_{A2}, \sigma_2)]_0^0$$

$$T^{(1)} = 2 \sum_{\sigma_1, \sigma_2, \sigma_p} \int d\xi_A d\mathbf{r}_{IA} d\mathbf{r}_{p1} d\mathbf{r}_{A2} \psi_A(\xi_A) \sum_{l_i, j_i} [\phi_{l_i, j_i}^{A+2}(\mathbf{r}_{A1}, \sigma_1, \mathbf{r}_{A2}, \sigma_2)]_0^{0*} \\ \times \chi_{PB}^{(-)*}(\mathbf{r}_{PB}) \chi_{m_i}^{1/2*}(\sigma_p) v(\mathbf{r}_{p1}) \phi_i(\mathbf{r}_{p1}, \sigma_1, \mathbf{r}_{p2}, \sigma_2) \chi_{m_i}^{1/2}(\sigma_p) \psi_A(\xi_A) \chi_{IA}^{(+)}(\mathbf{r}_{IA}) \\ = 2 \sum_{\sigma_1, \sigma_2, \sigma_p} \int d\mathbf{r}_{IA} d\mathbf{r}_{p1} d\mathbf{r}_{A2} \sum_{l_i, j_i} [\phi_{l_i, j_i}^{A+2}(\mathbf{r}_{A1}, \sigma_1, \mathbf{r}_{A2}, \sigma_2)]_0^{0*} \\ \times \chi_{PB}^{(-)*}(\mathbf{r}_{PB}) \chi_{m_i}^{1/2*}(\sigma_p) v(\mathbf{r}_{p1}) \phi_i(\mathbf{r}_{p1}, \sigma_1, \mathbf{r}_{p2}, \sigma_2) \chi_{m_i}^{1/2}(\sigma_p) \chi_{IA}^{(+)}(\mathbf{r}_{IA})$$

Check
With Eqs.
(5.1.4)

(5.1.5a)

Figure 3.1.1: Contribution of simultaneous transfer, in first order DWBA, to the reaction $A(t, p)B(\equiv A + 2)$. The nucleus A is schematically assumed to contain four nucleons, the triton being composed of two neutrons and one proton. The set of coordinates used to describe the entrance and exit channels are shown in the upper part (bold face vectors represent the coordinates used to describe the relative motion, while the intrinsic coordinates ξ_A represent \mathbf{r}_{34} , \mathbf{r}_{56} and \mathbf{r}_{34-56}). While in the lower part, the simultaneous two-nucleon transfer amplitude is written in detail (cf. Potel, G. et al. (2013b)). It is of notice that the expression of $T^{(1)}$ violates, in the independent particle basis used, the two-nucleon transfer sum rule by $T_{NO}^{(1)}$, amplitude operative also in lowest order of v (Fig. 3.1.2; see also App. 5.C). It is of notice that of all the relative motion coordinates, only those describing the relative motion of (t, A) and of (p, B) have asymptotic values, being those associated with distorted waves.

while

In

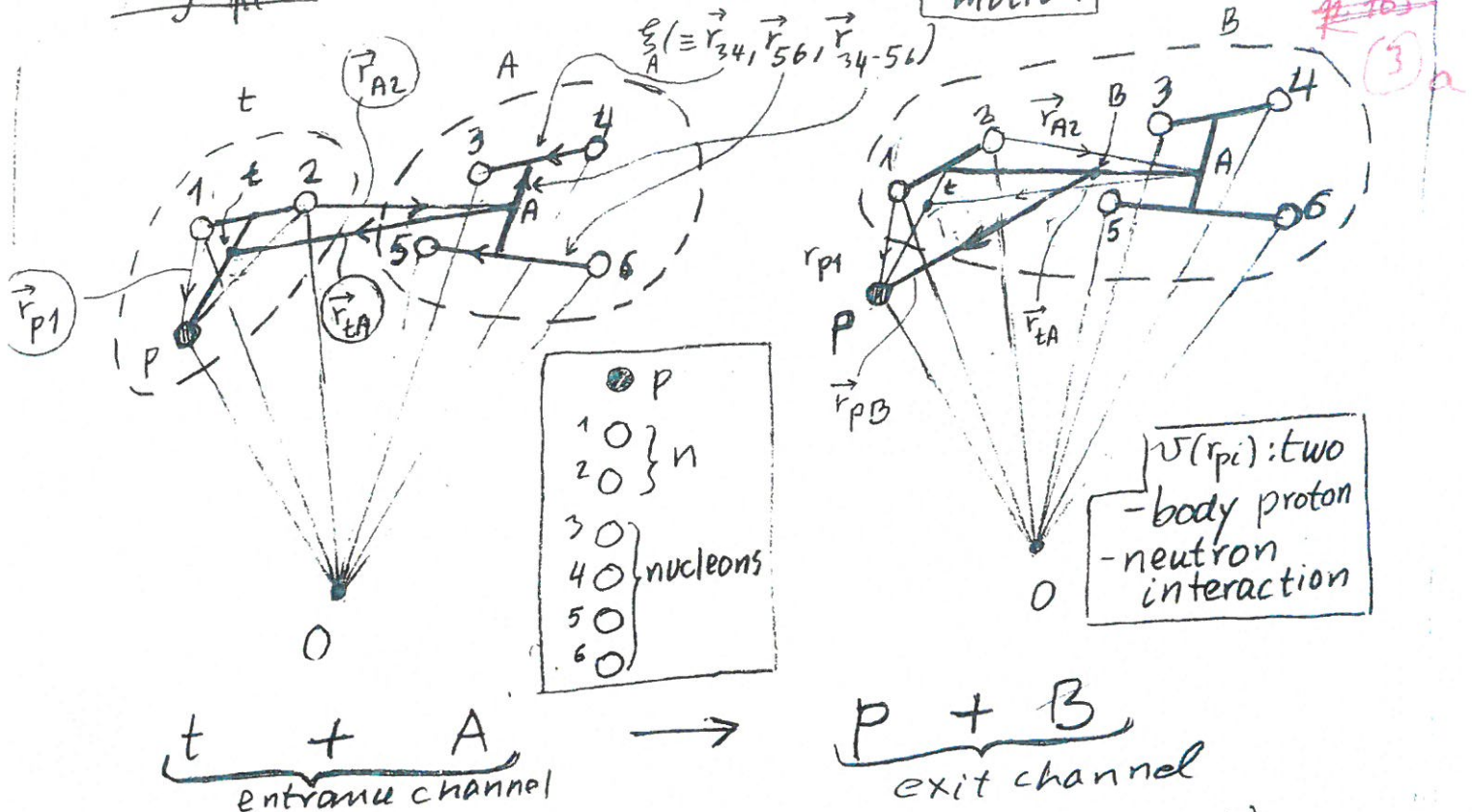
Check Ricardo
also Gregory

of the figure,

Fig. 3.1.1

6 coordinates of relative motion

#165
(3) a



$$\Phi_t(\vec{r}_{p1}, \sigma_1, \vec{r}_{p2}, \sigma_2) \chi_{m_s}^{1/2}(\sigma_p) \psi_A(\xi_A) \chi_{tA}^{(+)}(\vec{r}_{tA}) \\ (\Phi_d(r_{p1}, \sigma_1) \phi_d(r_{p2}, \sigma_2) \chi_{m_s}^{1/2}(\sigma_p) \psi_A(\xi_A) \chi_{tA}^{(+)}(\vec{r}_{tA}))$$

$$\Psi_B(\xi_A, \vec{r}_{A1}, \sigma_1, \vec{r}_{A2}, \sigma_2) = \Psi_A(\xi_A) \sum_{\ell_1, j_1} [\Phi_{\ell_1, j_1}^{A+2}(\vec{r}_{A1}, \sigma_1, \vec{r}_{A2}, \sigma_2)]_0^0 \\ = \Psi_A(\xi_A) \sum_{nm} a_{nm} [\Phi_{n, j_1}^{A+2}(\vec{r}_{A1}, \sigma_1) \Phi_{m, j_2}^{A+2}(\vec{r}_{A2}, \sigma_2)]_0^0$$

First order in v

$$(1) = \sum_{\sigma_1, \sigma_2} \int d\xi_A d^3r_{tA} d^3r_{p1} \sqrt{\psi_A^*(\xi_A)} \sum_{\ell_1, j_1} [\Phi_{\ell_1, j_1}^{A+2}(\vec{r}_{A1}, \sigma_1, \vec{r}_{A2}, \sigma_2)]_0^0 \chi^{(-)*}(\vec{r}_{PB}) \chi_{m_s}^{1/2}(\sigma_p) \mathcal{V}(\vec{r}_{p1}) \\ \times \Phi_t(\vec{r}_{p1}, \sigma_1, \vec{r}_{p2}, \sigma_2) \chi_{m_s}^{1/2}(\sigma_p) \psi_A(\xi_A) \chi_{tA}^{(+)}(\vec{r}_{tA})$$

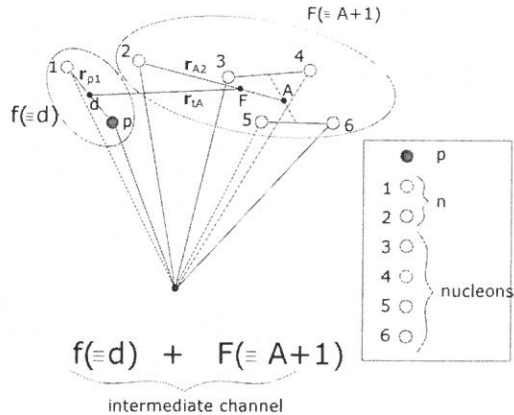
$$= 2 \sum_{\ell_1, j_1} \int d\xi_A d^3r_{tA} d^3r_{p1} d^3r_{A2} [\Phi_{\ell_1, j_1}^{A+2}(\vec{r}_{A1}, \sigma_1, \vec{r}_{A2}, \sigma_2)]_0^0 \chi^{(-)*}_{PB}(\vec{r}_{PB}) \mathcal{V}(\vec{r}_{p1}) \\ \times \Phi_t(\vec{r}_{p1}, \sigma_1, \vec{r}_{p2}, \sigma_2) \chi_{tA}^{(+)}(\vec{r}_{tA})$$

Notice that the above expression violates two-nucleon sum rule transfer (i.e., it transfers more than two neutrons) by exactly $T_{NO}^{(1)}$, operative also in the independent particle limit.

See scanning original figure bold-face vectors

$$\vec{1-p}, \vec{d-F}, \vec{r_{A2}}, (\vec{5-6}), \vec{3-4}$$

Check formulae in detail, compare with those at the beginning of CH 5, as well as with those of PRC on Sn



$$\begin{aligned}
 & \chi_{m_s}^{1/2}(\sigma_p) \phi_d(\mathbf{r}_{p1}, \sigma_1) \psi_A(\xi_A) \varphi_{l_f, j_f, m_f}^{A+1}(\mathbf{r}_{A2}, \sigma_2) \\
 G(\mathbf{r}_{dF}, \mathbf{r}'_{dF}) &= i \sum_l \sqrt{2l+1} \frac{f_l(k_{dF}, r_{<}) g_l(k_{dF}, r_{>})}{k_{dF} r_{dF} r'_{dF}} [Y^l(\hat{r}_{dF}) Y^l(\hat{r}'_{dF})]_0^0 \\
 T_{\text{succ}}^{(2)} &= 2 \sum_{l_i, j_i} \sum_{l_f, j_f, m_f} \sum_{\sigma_1 \sigma_2} \int d\xi_A dr_{dF} dr_{p1} dr_{A2} \chi_{pB}^{(-)*}(\mathbf{r}_{pB}) \chi_B^*(\xi_B) v(\mathbf{r}_{p1}) \phi_d(\mathbf{r}_{p1}) \varphi_{l_f, j_f, m_f}^{A+1}(\mathbf{r}_{A2}, \sigma_2) \\
 & \times \chi_{IA}^{(+)}(\mathbf{r}_{IA}) \psi_A^*(\xi_A) v(\mathbf{r}'_{p2}) \phi_d(\mathbf{r}'_{p1}) \varphi_{l_f, j_f, m_f}^{A+1}(\mathbf{r}'_{A2}, \sigma'_2) \\
 &= 2 \sum_{l_i, j_i} \sum_{l_f, j_f, m_f} \sum_{\sigma_1 \sigma_2} \int dr_{dF} dr_{p1} dr_{A2} \chi_{pB}^{(-)*}(\mathbf{r}_{pB}) v(\mathbf{r}_{p1}) \phi_d(\mathbf{r}_{p1}) [\varphi_{l_f, j_f, m_f}^{A+2}(\mathbf{r}_{A1}, \sigma_1, \mathbf{r}_{A2}, \sigma_2)]_0^0 \\
 & \times \frac{2\mu_{dF}}{\hbar^2} \int dr'_{dF} dr'_{p1} dr'_{A2} G(\mathbf{r}_{dF}, \mathbf{r}'_{dF}) \chi_{IA}^{(+)}(\mathbf{r}'_{IA}) v(\mathbf{r}'_{p2}) \phi_d(\mathbf{r}'_{p1}, \sigma'_1) \phi_d(\mathbf{r}'_{p2}, \sigma'_2) \varphi_{l_f, j_f, m_f}^{A+1}(\mathbf{r}'_{A2}, \sigma'_2)
 \end{aligned}$$

$$\begin{aligned}
 T_{NO}^{(1)} &= 2 \sum_{l_i, j_i} \sum_{l_f, j_f, m_f} \sum_{\sigma_1 \sigma_2} \int d\xi_A dr_{dF} dr_{p1} dr_{A2} \chi_{pB}^{(-)*}(\mathbf{r}_{pB}) \chi_B^*(\xi_B) v(\mathbf{r}_{p1}) \phi_d(\mathbf{r}_{p1}) \varphi_{l_f, j_f, m_f}^{A+1}(\mathbf{r}_{A2}, \sigma_2) \\
 & \times \chi_{m_s}^{1/2}(\sigma_p) \Psi_A(\xi_A) \frac{2\mu_{dF}}{\hbar^2} \int d\xi'_A dr'_{dF} dr'_{p1} dr'_{A2} \\
 & \times \chi_{IA}^{(+)}(\mathbf{r}_{IA}) \psi_A^*(\xi_A) \phi_d(\mathbf{r}'_{p1}) \varphi_{l_f, j_f, m_f}^{A+1}(\mathbf{r}'_{A2}, \sigma'_2) \\
 &= 2 \sum_{l_i, j_i} \sum_{l_f, j_f, m_f} \sum_{\sigma_1 \sigma_2} \int dr_{dF} dr_{p1} dr_{A2} \chi_{pB}^{(-)*}(\mathbf{r}_{pB}) v(\mathbf{r}_{p1}) \phi_d(\mathbf{r}_{p1}) [\varphi_{l_f, j_f, m_f}^{A+2}(\mathbf{r}_{A1}, \sigma_1, \mathbf{r}_{A2}, \sigma_2)]_0^0 \\
 & \times \frac{2\mu_{dF}}{\hbar^2} \int dr'_{dF} dr'_{p1} dr'_{A2} \chi_{IA}^{(+)}(\mathbf{r}'_{IA}) \phi_d(\mathbf{r}'_{p1}, \sigma'_1) \phi_d(\mathbf{r}'_{p2}, \sigma'_2) \varphi_{l_f, j_f, m_f}^{A+1}(\mathbf{r}'_{A2}, \sigma'_2)
 \end{aligned}$$

Check with (5.1.5b)
and (5.1.5c)

(corresponding to the (t,p) process)

Figure 3.1.2: Successive and non-orthogonality contributions to the amplitude describing two-nucleon transfer in second order DWBA, entering in the expression of the absolute differential cross section $d\sigma/d\Omega = \frac{\mu_{dF}}{(4\pi\hbar^2)^2} \frac{k_F}{k_i} |T^{(1)} + T_{\text{succ}}^{(2)} - T_{NO}^{(1)}|^2$.

Concerning $T^{(1)}$ we refer to Fig. 3.1.1. In the upper part of the figure the coordinates used to describe the intermediate channel $d + F (\equiv A + 1)$ are given

(bold face vectors represent the coordinates used to describe the relative motion,

while the intrinsic coordinates ξ_A represent \mathbf{r}_{34} , \mathbf{r}_{56} and \mathbf{r}_{34-56}) while in the

lower part, the responding expressions are displayed (Potel, G. et al., 2013b).

In the case of a (t, p) process. Schematically, the three contributions $T^{(1)}$, $T_{\text{succ}}^{(2)}$ and

$T_{NO}^{(1)}$ to the transfer amplitude can be written as $\langle pB|v|tA \rangle$, $\sum \langle pB|v|dF \rangle \langle dF|v|tA \rangle$ and

$\sum \langle pB|v|dF \rangle \langle dF|1|tA \rangle$ respectively, where v is the proton-neutron interaction and 1 the unit operator. Within this context, while $T_{NO}^{(1)}$ receives contributions from the intermediate (virtual) closed $(d + F)$ channel as $T_{\text{succ}}^{(2)}$ does, it is first order in v as $T^{(1)}$.

while

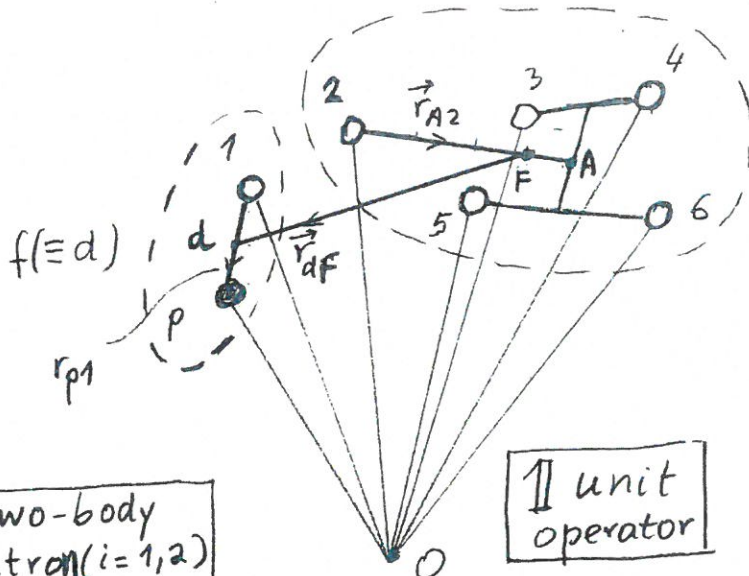
of the figure

Fig. 3.1.2

Fig. 3.1.2

$F (\equiv A+1)$

(4) a



$V(r_{pi})$: two-body proton-neutron ($i=1,2$) interaction

$f (\equiv d) + F (\equiv A+1)$
intermediate channel

P	
1 O	$\} n$
2 O	
3 O	
4 O	
5 O	nucleons
6 O	

no distorted wave
 $as(f, F)$ is a virtual
channel with no
asymptotic waves.
thus 5 relative
coordinates

$$\chi_{m_s(\sigma_p)}^{1/2} \phi_d(\vec{r}_{p1}, \sigma_1) \psi(\xi_A) \varphi_{l_f j_f m_f}^{A+1}(\vec{r}_{A2}, \sigma_2)$$

$$T^{(2)}_{\text{succ}} = 2 \sum_{\substack{\ell_i j_i, \ell_f j_f m_f, m_s, m_s' \\ \sigma_i \sigma_i' \sigma_i' \sigma_i' \\ \sigma_i \sigma_i' \sigma_i' \sigma_i'}} S d^3 r_{dF} d^3 r_{p1} d^3 r_{A2} \chi_{pB}^{(-)*}(\vec{r}_{pB}) \chi_{m_s(\sigma_p)}^{1/2*} \chi_B^{(\xi_B)} V(r_{p1}) \phi_d(r_{p1}, \sigma_1) \varphi_{\ell_f j_f m_f}^{A+1}(\vec{r}_{A2}, \sigma_2) \chi_{m_s'(\sigma_p)}^{1/2} \psi_A(\xi_A)$$

$$\times \frac{2 \mu_{dF}}{\hbar^2} \int d^3 r_{p1}' d^3 r_{A2}' d^3 r_{dF}' G(\vec{r}_{dF}, \vec{r}_{dF}') \chi_{m_s'(\sigma_p')}^{1/2*} \phi_d^{*}(r_{p1}', \sigma_1') \psi(\xi_A') \varphi_{\ell_f j_f m_f}^{A+1}(\vec{r}_{A2}', \sigma_2') V(r_{p2}')$$

$$\times \phi_t(r_{p1}', \vec{r}_{p2}', \sigma_2') \chi_{m_s'(\sigma_p')}^{1/2} \psi_A(\xi_A') \chi_{tA}^{(+)}(\vec{r}_{pA})$$

$$= 2 \sum_{\substack{\ell_i j_i, \ell_f j_f m_f \\ \sigma_i \sigma_i' \sigma_i' \sigma_i' \\ \sigma_i \sigma_i' \sigma_i' \sigma_i'}} S d^3 r_{dF} d^3 r_{p1} d^3 r_{A2} \chi_{pB}^{(-)*}(\vec{r}_{pB}) [\varphi_{\ell_i j_i}^{A+2}(\vec{r}_{A1}, \sigma_1, \vec{r}_{A2}, \sigma_2)]_0^0 V(r_{p1}) \phi_d(r_{p1}, \sigma_1) \varphi_{\ell_f j_f m_f}^{A+1}(\vec{r}_{A2}, \sigma_2)$$

$$\times \frac{2 \mu_{dF}}{\hbar^2} \int d^3 r_{p1}' d^3 r_{A2}' d^3 r_{dF}' G(\vec{r}_{dF}, \vec{r}_{dF}') \phi_d^{*}(r_{p1}', \sigma_1') \varphi_{\ell_f j_f m_f}^{A+1}(\vec{r}_{A2}', \sigma_2') V(r_{p2}') \phi_d(r_{p1}', \sigma_1') \phi_d(r_{p2}', \sigma_2') \chi_{tA}^{(+)}(\vec{r}_{pA})$$

First order in v

$$T^{(1)}_{\text{NO}} = 2 \sum_{\substack{\ell_i j_i, \ell_f j_f m_f \\ m_s m_s' \\ \sigma_i \sigma_i' \\ \sigma_i \sigma_i' \sigma_i' \sigma_i' \\ \sigma_i \sigma_i' \sigma_i' \sigma_i'}} S d^3 r_A d^3 r_{dF} d^3 r_{p1} d^3 r_{A2} \chi_{pB}^{(-)*}(\vec{r}_{pB}) \chi_{m_s(\sigma_p)}^{1/2*} \psi_B^{*(\xi_B)} V(r_{p1}) \phi_d(r_{p1}, \sigma_1) \varphi_{\ell_f j_f m_f}^{A+1}(\vec{r}_{A2}, \sigma_2) \chi_{m_s'(\sigma_p)}^{1/2} \psi_A(\xi_A)$$

$$\times \underbrace{\{ d^3 r_A d^3 r_{p1} d^3 r_{A2} d^3 r_{dF} \}}_{6 \text{ relative coords.}} \chi_{m_s'(\sigma_p')}^{1/2*} \phi_d^{*}(r_{p1}', \sigma_1') \psi(\xi_A') \varphi_{\ell_f j_f m_f}^{A+1}(\vec{r}_{A2}', \sigma_2') \mathbb{I} \phi_t(r_{p1}', \vec{r}_{p2}', \sigma_2') \psi_A(\xi_A') \chi_{tA}^{(+)}(\vec{r}_{pA})$$

$$= 2 \sum_{\substack{\ell_i j_i, \ell_f j_f m_f \\ m_s m_s' \\ \sigma_i \sigma_i' \\ \sigma_i \sigma_i' \sigma_i' \sigma_i' \\ \sigma_i \sigma_i' \sigma_i' \sigma_i'}} d^3 r_{dF} d^3 r_{p1} d^3 r_{A2} \chi_{pB}^{(-)*}(\vec{r}_{pB}) [\varphi_{\ell_i j_i}^{A+2}(\vec{r}_{A1}, \sigma_1, \vec{r}_{A2}, \sigma_2)]_0^0 V(r_{p1}) \phi_d(r_{p1}, \sigma_1) \varphi_{\ell_f j_f m_f}^{A+1}(\vec{r}_{A2}, \sigma_2)$$

$$\times \int d^3 r_{p1}' d^3 r_{A2}' d^3 r_{dF}' \phi_d^{*}(r_{p1}', \sigma_1') \varphi_{\ell_f j_f m_f}^{A+1}(\vec{r}_{A2}', \sigma_2') \mathbb{I} \phi_t(r_{p1}', \sigma_1') \phi_d(r_{p2}', \sigma_2') \chi_{tA}^{(+)}(\vec{r}_{pA})$$

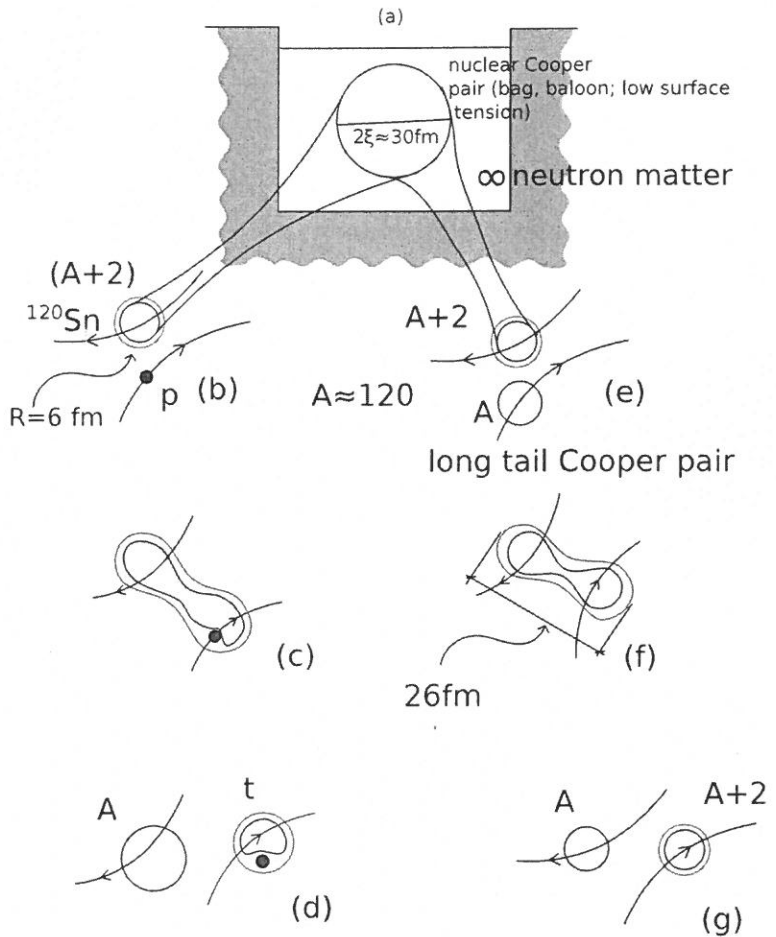
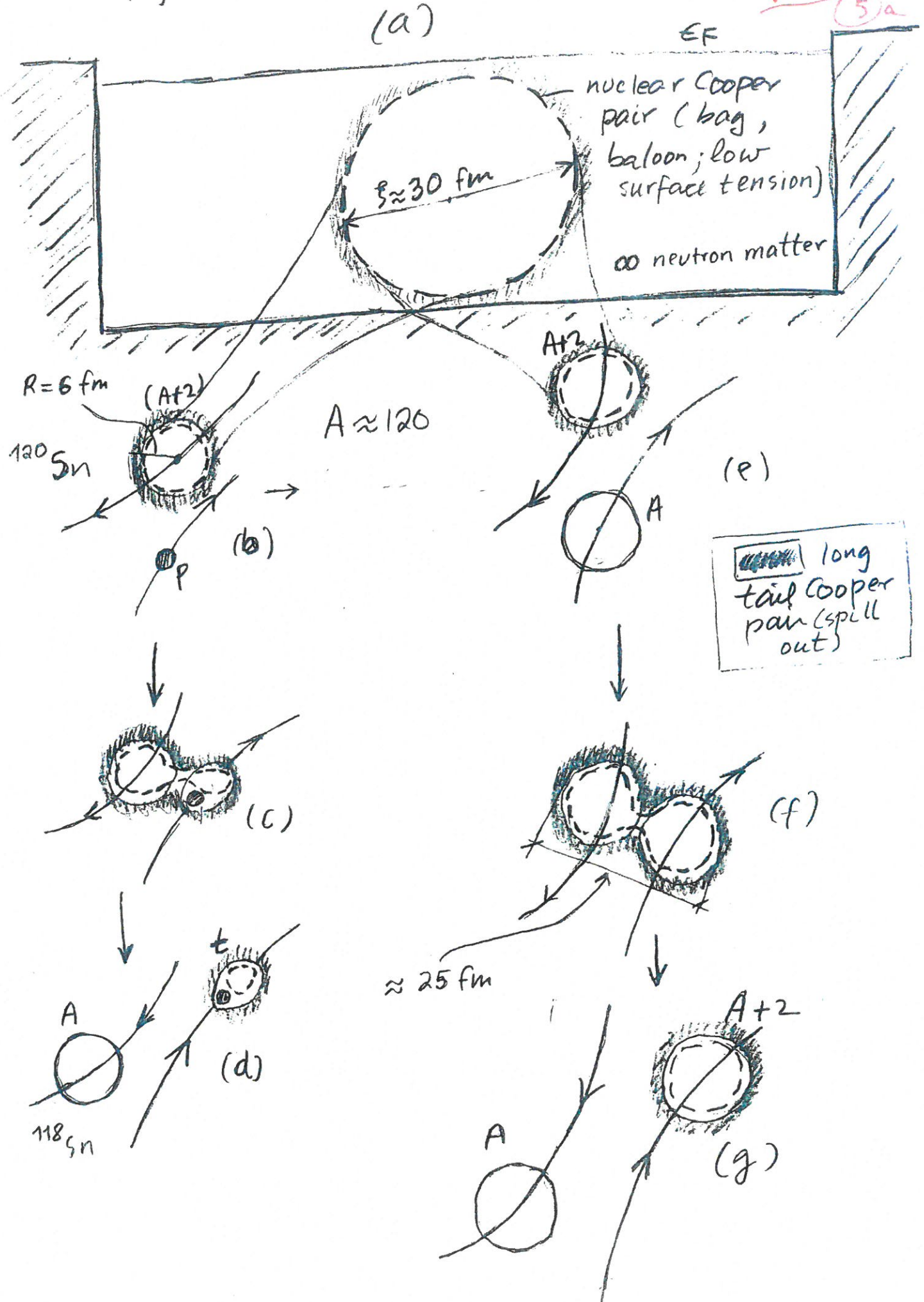


Figure 3.1.3: The correlation length associated with a nuclear Cooper pair is of the order of $\xi \approx \hbar v_F / (\pi \Delta) \approx 14$ fm. (a) in neutron matter at typical densities of the order of 0.5–0.8 saturation density, the $NN^{-1}S_0$ short range force, eventually renormalized by medium polarization effects, makes pairs of nucleons moving in time reversal states to correlate over distances larger than nuclear dimensions. How can one get evidence for such an extended object? Hardly when the Cooper bag (balloon) is introduced in (b) the mean field of a superfluid nucleus which, acting as a very strong external field, constrains the Cooper pair to be within the nuclear radius with some spill out (long tail of Cooper pair, grey, shaded area extending outside the nuclear surface defined by $R_0 = 1.2A^{1/3}$ fm; see also Bertsch and Broglia (2005) p. 88), (d), that is, in the case of two-nucleon transfer process (e.g. (p, t) reaction) in which the absolute cross section can change by orders of magnitude in going from pure two-particle (uncorrelated configurations) to long tail Cooper pair spill outs. This effect is expected to become stronger by allowing pair transfer between similar superfluid nuclei, in which case one profits of the same type of correlations (superfluidity) as resulting from very similar pair mean fields (e), (f), (g) (see e.g. von Oertzen, W. (2013); von Oertzen and Vitturi (2001), and references therein).

Fig. 3.1.3



Because typical values of the absolute one-particle cross section associated with the (p, d) reaction mentioned above are few mb (see e.g. Fig. 4.2.3 right panel) one can use, for order of magnitude estimate purposes,

$$P_1 \approx \frac{5.35 \text{ mb}}{2.7 \text{ b}} \approx 10^{-3}, \quad (3.2.18)$$

as the typical probability for such processes. Consequently, one may argue that the probability for a pair of nucleons to simultaneously tunnel in e.g. the (p, t) process mentioned above is $(P_1)^2 \approx 10^{-6}$, as near impossible as no matter. Within this context we note that the integrated $\text{gs} \rightarrow \text{gs}$ absolute cross section $\sigma(^{120}\text{Sn}(p, t)^{118}\text{Sn}(\text{gs})) \approx 2.25 \pm 0.338 \text{ mb}$ (see Figs. 2.1.3, 2.1.6 and 6.4.1). This fact implies that the empirical two-nucleon transfer probability is of the order of $P_2 \approx 10^{-3}$. Consequently, $P_2/(P_1)^2 \approx 10^3$, a ratio which, again, can hardly be explained in terms of a physical enhancement factor.

The above contradictions¹³ are, to a large extent, connected with the fact that one is addressing the subject of pairing correlations in nuclei as probed by two-nucleon transfer reactions, treating separately the associated questions of structure and reactions, while they are but complementary aspects of the same physics. Let us elaborate on this point.

When one turns on, in an open shell atomic nucleus like e.g. $^{120}_{50}\text{Sn}_{70}$, a pairing interaction of strength larger than critical, the system moves into an independent pair regime¹⁴. This fact has essentially no consequence concerning the one-particle transfer mechanism, exception made regarding the size of the mismatch between the relative motion–incoming ($p + ^{120}\text{Sn}(\text{gs})$) and –outgoing ($d + ^{119}\text{Sn}(\text{gs})$) trajectories (Q -value and recoil effect), in keeping with the fact that one has to break a Cooper pair to populate a single quasiparticle state. From a structure point of view the depletion of the occupation probability measured in a (p, d) process is correlated with the corresponding increase in occupation observed in (d, p) (U^2, V^2 factors). Aside from the quantitative values, this is also observed in dressed single-particle states, the single-particle sum rule implying both the (A-1) and (A+1) system (see App. 4.H). Concerning the phase coherence of the pair correlated wavefunction it has no consequence for one-particle transfer process, in keeping with the fact that $|e^{i\phi} \sqrt{P_1}|^2 = P_1$.

The situation is very different concerning (Cooper) pair transfer. From a reaction point of view, and in keeping with the non-orthogonality existing between the

¹³Within this context it is of notice that similar questions were raised by Bardeen (1962, 1961); Pippard (2012); Cohen et al. (1962); McDonald (2001) in connection with the prediction of Josephson (Josephson (1962)) that there should be a contribution to the current through an insulating barrier between two superconductors which would behave like direct tunneling of condensed pairs. This is in keeping with the fact that a single electron had a probability of $\approx 10^{-10}$ of getting through, the “classical” estimate of simultaneous pair tunneling being $\approx 10^{-20}$, an impossible observation.

¹⁴Regime which is conditioned by the “external” mean field. In other words, regime (abnormal density) which express itself provided there is nucleon (normal) density available. It is of notice that pairing in turn may help extend the range over which normal nucleon density is available, as in the case of the neutron halo nucleus ^{11}Li lying (defining) at the neutron drip line.

espectacular

A further evidence, if it was the need, that two-particle transfer is the specific probe of pairing in nuclei.

$$\exp\left(-\frac{\sqrt{2}r}{\xi}\right),$$

wavefunction can be written as¹⁷

$$F(r) \approx \Delta N(0) \frac{\sin k_F r}{k_F} \exp\left(-\frac{\sqrt{2}r}{\xi}\right), \quad (3.2.20)$$

where $N(0)$ is the density of levels at the Fermi energy for one spin orientation. For $r \leq \xi$ the pair wavefunction is approximately proportional to that of two particles at the Fermi energy moving freely in a relative s -wave state. In a typical metallic superconductor ξ is of the order of 10^4 Å, much larger than the inter electron spacing (≈ 2 Å). Note that relative to the Fermi energy, the correlation energy ($E_{corr} = (-1/2)\Delta N(0)\Delta^2$) associated with Cooper pairing is very small, $\approx 10^{-7} - 10^{-8}$. Arguably, the most important consequence of this fact, is the exponentially large radius and thus very small value of the relative momentum associated with Cooper pairs. In other words, the typical scenario for a very small value of the localization kinetic energy and thus of the generalized quantality parameter (cf. App. 6.E), implying that the two partners, are rigidly anchored to each other (Cooper pair). This phenomenon is at the basis of the emergence of new elementary modes of excitation (pairing vibrations for single Cooper pairs, pairing rotations for few ones, supercurrents and Josephson currents for macroscopic amounts of them).

The situation of very extended Cooper pairs sound, in principle, very different in the case of condensed matter (e.g. low-temperature superconductors) than in atomic nuclei, in keeping with the fact that nuclear Cooper pairs are, as a rule, subject to an overwhelming external (mean) field ($|E_{corr}| \approx 2\Delta \approx 2.4$ MeV $\ll |U(r \approx R_0)| \approx |V_0/2| \approx 25$ MeV). But even in this case, one can posit that in the transition from independent-particle to independent-pair motion implies that Cooper pair partners recede from each other. Let us clarify this point for the case of a single pair, e.g. $^{210}\text{Pb(gs)}$. It is true that allowing the pair of neutrons to correlate in the valence orbitals leads to a pair wavefunction which is angle correlated ($\Omega_{12} \approx 0$), as compared to the pure $j^2(0)(j = g_{9/2})$ configuration¹⁸ (App. 3.D). On the other hand, the correlated pair addition mode (Tables 2.5.4 and 2.5.5) will display a sizeable spill out as compared to the pure two particle state, and thus a lower density and larger related average distance between Cooper pair partners. This is also the reason why close to $\approx 40\%$ of the pairing matrix elements is contributed by the induced pairing interaction resulting from the exchange of long wavelength, low-lying, collective modes, the other $\approx 60\%$ resulting from the bare nucleon-nucleon 1S_0 pairing interaction. In carrying out the above arguments the values of $(|E_{corr}|/\epsilon_F)^2 \approx \left(\frac{2.4\text{ MeV}}{36\text{ MeV}}\right)^2 \approx 10^{-3}$ and $\xi = \frac{\hbar v_F}{\pi\Delta} \approx 14$ fm ($(\frac{v_F}{c}) \approx (k_F)_{\text{fm}^{-1}}/5 \approx 0.27$), typical for superfluid nuclei lying along the stability valley, were used.

The situation described above becomes likely clearer, even if extreme, in the case of ^{11}Li . In this case, the Fermi momentum is $k_F \approx 0.8\text{ fm}^{-1}$, the radius $R \approx 4.58\text{ fm}$, much larger than $R_0 = 2.7\text{ fm}$ expected from systematics. Furthermore essentially all of the correlation energy ($E_{corr} \approx -0.5$ MeV, $(E_{corr}/\epsilon_F)^2 \approx$

¹⁷cf. Leggett (2006) p. 185; for the non local nuclear version cf. e.g. Broglia and Winther (1983).

¹⁸Bertsch, G. F. et al. (1967), Ferreira, L. et al. (1984); Matsuo, M. (2013).

3.2.1 Interplay between mean field and correlation length

In Fig. 3.2.1 one displays a schematic representation of two possible *gedanken experiments* situations: (a) (*independent particle motion*) system which can be probed in a (p, t) reaction leading insight into non-interacting nucleons confined in a mean field potential, e.g. a Saxon-Woods potential with standard parametrization²⁰; (b) (*independent pair motion*), target of pickup reactions induced in a heavy ion collision between superfluid nuclei, in which nucleons interacting through an effective pairing interaction, sum of a short (v_p^{bare}) and long range (v_p^{ind}) NN -pairing potential, confined by a mean field whose parameters are freely adjusted so as to profit at best the pair coupling scheme.

In other words, one moves from a situation in which one assumes: (a) $H = T + v \approx T + U$ (ansatz $\langle v - U \rangle \approx 0$) to another in which (b) $H = T + v \approx T + U' + v_p^{eff}$ (ansatz $\langle v - U' - v_p^{eff} \rangle \approx 0$ and $|U'| \lesssim |U|$, $|v_p^{eff}| \ll |U'|$). Switching from the first to the second situation pairs of nucleons moving in time reversal states will tend to recede from each other. It can be argued that, to the extent that one is interested in describing nuclei lying along the stability valley like e.g. ^{120}Sn , could posit that the ansatz (a) is more realistic than (b), in keeping with the fact that $(U' + v_p^{eff})$ represent a much smaller fraction of v than U does. Consequently, the right view seems to be that of (a) plus pairing, in which case Cooper pair partners approach each other, if nothing else, because of angular correlation²¹ (App. 3.D). Now, this result may be interesting in itself in order to compare (nuclear structure) theory with theory, but not theory with experiment at least not the experiments associated with the specific probe of Cooper pair correlations, namely two-nucleon transfer reactions, in which case the closest quantity to be observable is the two-nucleon transfer formfactor (Sect. 6.6.3).

The “correctness” of picture (b) gets strong support from the fact that one- and two-particle transfer absolute cross sections have the same order of magnitude²².

Within this context we note that the fact that $^9_3\text{Li}_6$ is well bound ($N = 6$ isotope parity-inverted closed shell), $^{10}_3\text{Li}_7$ is not while $^{11}_3\text{Li}_8$ is again bound, indicates that we are confronted with a pairing phenomenon. Allowing the two neutrons moving outside $N = 6$ closed shell to correlate in the configurations $j^2(0)(s_{1/2}^2, p_{1/2}^2, d_{5/2}^2 \dots)$ through a short range bare pairing interaction, e.g. the v_{14} Argonne NN -potential, does not lead to a bound state. The system lowers the relative momentum of the pair by exchanging at the same time the low-lying dipole vibration of the associated diffuse system becoming, eventually, bound, ever so weakly ($S_{2n} = 380$ MeV). The radius of the resulting system ($R(^{11}\text{Li}) = 4.58 \pm 0.13$ fm) corresponds, in the parametrization $R_0 = 1.2A^{1/3}$ fm, to an effective mass

²⁰Bohr and Mottelson (1969)

²¹Bertsch, G. F. et al. (1967); Ferreira, L. et al. (1984); Matsuo, M. (2013) and refs. therein.

²²For example (Fortune et al. (1994)) $^{10}\text{Be}(t, p)^{12}\text{Be}(\text{gs})$ ($\sigma = 1.9 \pm 0.5$ mb, $4.4^\circ \leq \theta_{CM} \leq 54.4^\circ$) as compared to (Schmitt et al. (2013)) $^{10}\text{Be}(d, p)^{11}\text{Be}(1/2^+)$ ($\sigma = 2.4 \pm 0.013$ mb, $5^\circ \leq \theta_{CM} \leq 39^\circ$) in the case of light nuclei around closed shell, and (Bassani et al. (1965)) $^{120}\text{Sn}(p, t)^{118}\text{Sn}(\text{gs})$ ($\sigma = 3.024 \pm 0.907$ mb, $5^\circ \leq \theta_{CM} \leq 40^\circ$) as compared to (Bechara, M. J. and Dietzsch (1975)) $^{120}\text{Sn}(d, p)^{121}\text{Sn}(7/2^+)$ ($\sigma = 5.2 \pm 0.6$ mb, $2^\circ \leq \theta_{CM} \leq 58^\circ$).

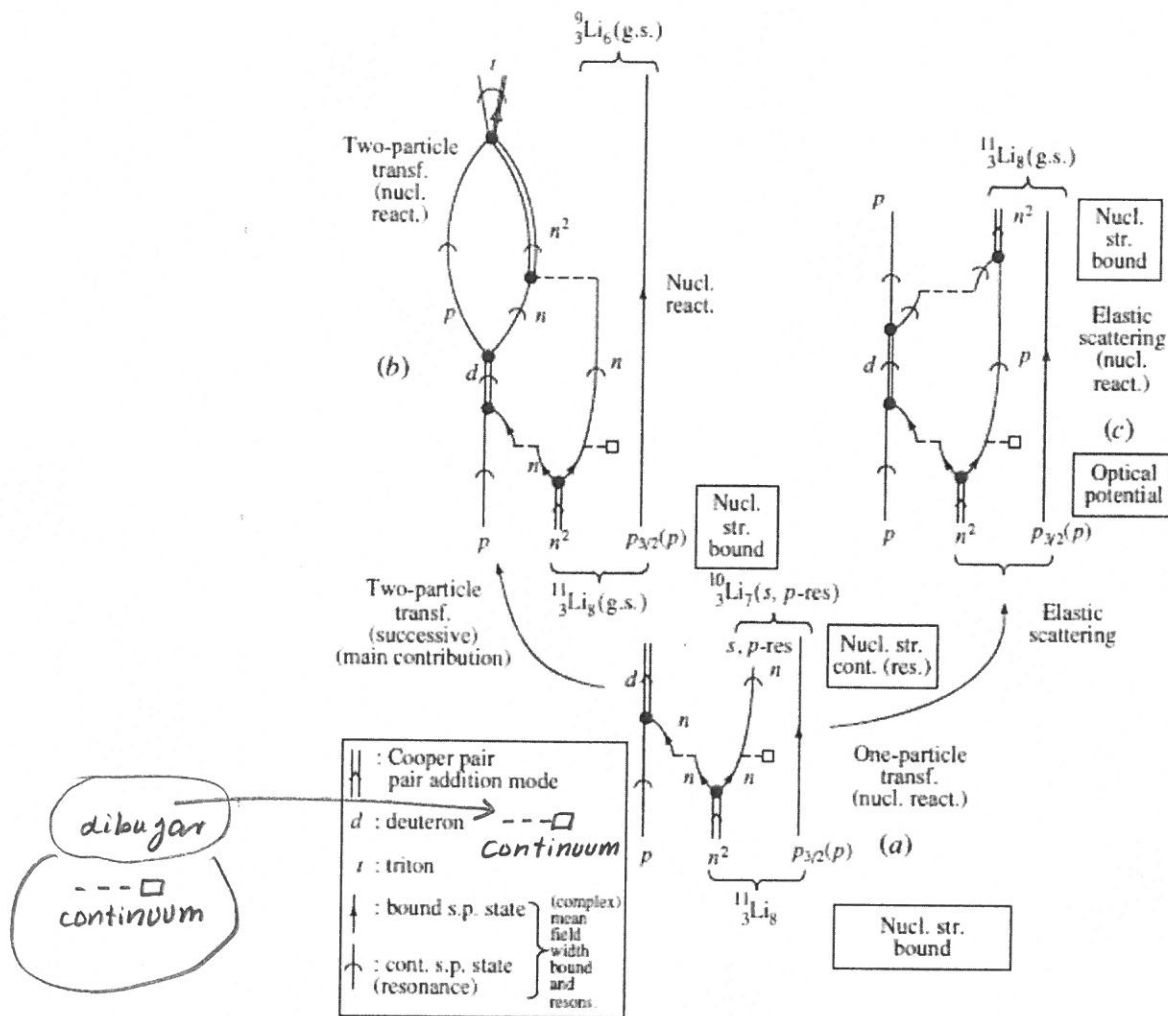


Figure 3.5.3: Simplified NFT diagrams summarizing the physics which is at the basis of the structure of ^{11}Li (Barranco, F. et al. (2001)) and of the analysis of the $^{11}\text{Li}(p,t)^9\text{Li}(\text{g.s.})$ reaction (Potel et al. (2010)). In the figure emphasis is set on intermediate (like, e.g., $^{10}\text{Li}+d$, see (a) and (b)) and elastic (see (c), see also Fig. 3.5.4) channels. It is of notice that for simplicity the recoil mode has not been drawn (within this connection see Figs. 1.9.2 and 1.9.3).

where \Re stands for real part. Making use of

$$\sum_k \rightarrow N_1 \int d\epsilon_1, \quad \sum_q \rightarrow N_2 \int d\epsilon_2 \quad (3.6.18)$$

where N_1 and N_2 are the density of levels of one spin at the Fermi energy one finally obtains⁴⁹

$$\begin{aligned} \Delta E_2 &\approx -N_1 N_2 \Delta_1 \Delta_2 \langle |T_{kq}|^2 \rangle \cos(\phi_1 - \phi_2) \int_{-\infty}^{\infty} \int_{-\infty}^{\infty} \frac{d\epsilon_1 d\epsilon_2}{E_1 E_2 (E_1 + E_2)} \\ &\approx -2\pi N_1 N_2 \langle |T_{kq}|^2 \rangle \cos(\phi_1 - \phi_2) \left(\pi \frac{\Delta_1 \Delta_2}{\Delta_1 + \Delta_2} \right). \end{aligned} \quad (3.6.19)$$

Consequently, the maximum possible supercurrent is the same as the normal current at an equivalent voltage⁵⁰

$$\checkmark V_{\text{equiv}} = \frac{\pi}{e} \frac{\Delta_1 \Delta_2}{(\Delta_1 + \Delta_2)}. \quad (3.6.20)$$

For two identical superconductors $V_{\text{equiv}} = \pi\Delta/(2e)$, the associated supercurrent being

$$\frac{\pi}{4} \frac{V_{\text{equiv}}}{R_n} \quad J_0 = \frac{\pi \Delta}{2e R_n} \quad (3.6.21)$$

where R_n is the tunneling resistance per unit area of the junction when both metals are in the normal state. For Pb and Sn, the gaps are 1.4 meV and 0.7 meV, leading to eV_{equiv} ($V_{\text{equiv}} \approx 2.0$ meV (2.0 mV) and 0.7 meV (0.7 mV) respectively. Assuming R_n to be of the order of 1Ω per unit area, implies maximum values of the Josephson supercurrent $J = J_0 \sin \gamma$ ($\gamma = \phi_0 - \phi_0 - \frac{2e}{\hbar c} \int_A \mathbf{A} \cdot d\mathbf{l}$, where A is the vector potential), of the order of $J_0 \approx 2$ mA as experimentally observed.

It is suggestive that the expression (3.6.20) is formally similar to that of the ion-ion potential acting between two heavy ions in weak contact, namely at a distance a diffusivity away from the grazing distance r_g . In this case the role of the reduced gap is played by a quantity closely related to the reduced radius of curvature⁵¹

$$U_{aa}^N(r_g + a) \sim \gamma \frac{R_a R_A}{R_a + R_A} a. \quad (3.6.22)$$

In the above expression $\gamma \approx 0.9$ MeV/fm² is the surface tension, $a = 0.63$ fm the diffusivity of the potential, $R_i (= (1.233 A^{1/3} - 0.98 A^{-1/3})$ fm) being the radii of nuclei

⁴⁹It is of notice that ΔE_2 is bilinear in the density of levels (see Potel et al. (2017)).

⁵⁰Tinkham (1996) Ch. 6, Eq. (6-4) and subsequent discussion; see also Anderson (1964a) Eq. (11) and following discussion.

⁵¹Broglia and Winther (2004) p.114 Eq. (40), $U_{aa}^N(r) = -V_0/(1 + \exp(\frac{r-R_0}{a}))$, $V_0 = 16\pi\gamma R_a a$, $R_0 = R_a + R_A + 0.29$ fm, which for two ¹²⁰Sn nuclei ($R = 5.883$ fm) leads to $R_0 \approx 12.1$ fm and $V_0 = 83.8$ MeV. For energies somewhat above the Coulomb barrier, the grazing distance (Eq. (25) p. 128) of the above reference is $r_g = r_B - \delta \approx 12.8$ fm ($r_B \approx 13.3$ fm, $\delta \approx 0.5$ fm). Thus $(1 + \exp(\frac{r_g + a - R}{a})) \approx 10.1$.

and $V_{\text{equiv}} = 2\Delta/e$ is the minimum voltage at which a normal current, upon breaking Cooper pairs, starts to flow.

it will fluctuate (QM, ZPF, Goldstone mode), and decay into a state

$$|N\rangle \sim \int d\phi e^{iN\phi} |BCS(\phi)\rangle_{\mathcal{K}} \sim \sum_{N'} \int_0^{2\pi} d\phi e^{-i(N'-N)\phi} |\Psi_{N'}\rangle \sim |\Psi_N\rangle \quad (3.7.26)$$

in keeping with the fact that

$$\int_0^{2\pi} d\phi e^{-i(N'-N)\phi} = \begin{cases} 2\pi\delta(N, N') & (N = N'), \\ \frac{i}{N'-N} e^{-i(N'-N)\phi} \Big|_0^{2\pi} = 0 & (N \neq N'). \end{cases} \quad (3.7.27)$$

Records
slab
scanning

$\otimes - \otimes$

pp,
 ^{256}Ca +
 ^{256}Ba

handwritten

The state $|\Psi_N\rangle$ is a member of a pairing rotational band around neutron mass number N : for example the ground states of the Sn-isotopes around $N_0 = 68$ (see Fig. 2.1.3). Because $E_R = (\hbar^2/2I)(N - N_0)^2 = (G/4)(N - N_0)^2 = G/4(\frac{1}{\phi})^2$ is the kinetic energy of rotation in (nuclear) gauge space, and $G/4 \approx 25/(4N_0) \approx 0.092$ MeV, the wavepacket (??) will decay⁵⁶ in the state (3.7.26) in a time of the order of $\hbar/(\hbar^2/2I) \approx \hbar/0.092$ MeV $\approx 10^{-20}$ s. More accurately, because $N = N_0 \pm 2$, $\hbar/E_R \approx \hbar/(4 \times 0.092 \text{ MeV}) \approx 2 \times 10^{-21}$ s. In other words, superfluid nuclei cannot be prepared, in isolation, in states with coherent superposition of different N -values. The common assumption that N is fixed, ϕ meaningless is correct.

This is also the case for real superconductors. In fact, the corresponding state (??) even if prepared in isolation would dissipate because there is a term in the energy of the superconductor depending on N , namely the electrostatic energy $e(N - N_0)^2/2C = e^2/2C(\partial/\partial\phi)^2$, where C is the electrostatic capacity. The system will dissipate, no matter how small $\delta\phi$ is. In fact, let us assume $\delta\phi = 1$ degree. The kinetic energy of rotation in gauge space is of the order of $(e^2/2C)(1/\delta\phi)^2$ (of notice that $\delta N\delta\phi/2\pi \sim 1$), and

$$\Delta E = \frac{1.44 \text{ fm MeV}}{1 \text{ cm } (1^\circ)^2} \sim 1.44 \times 10^{-13} \text{ MeV}, \quad (3.7.28)$$

which corresponds to an interval of time

$$\Delta t \approx \frac{\hbar}{1 \text{ MeV}} \frac{10^{13}}{1.44} \approx \frac{0.667 \times 10^{-21} \text{ sec}}{1.44} \times 10^{13} \approx 10^{-9} \text{ sec}. \quad (3.7.29)$$

The opposite situation is that of the case in which one considers different parts of the same superconductor. In this case one can define relative variables $n = N_1 - N_2$

⁵⁶Within this context note that setting in phase at $t = 0$ all the states in which a GDR breaks down through the hierarchy of doorway-states-coupling, they would dissipate like a wavepacket of free particles after 10^{-22} sec (assuming $\Gamma_{GDR} \approx 3 - 4$ MeV). It is of notice that the GDR will eventually branch into the ground state, although $\Gamma_g \ll \Gamma_{GDR}$, in keeping with the fact that the $t = 0$ phase coherent states are, individually, stationary. What is not stationary is its phase coherence (see Sect. 1.3). Pushing the analogy a step further, one can say that in quantum mechanics, while the outcome of an experiment is probabilistic the associated probability evolve in a deterministic way (Born (1926)). This is the reason why a large gamma ray detector will reveal a well defined peak of the resonant dipole state long after its lifetime deadline (\hbar/Γ). Also, one can obtain a completely (classical) picture of a face making use of single photons at a time, provided one waits long enough.

why

(8) The state $|N\rangle$ is a member of the pairing rotational band centered around neutron number N_0 . In the example discussed in connection with Figs. 2.1.2 and 2.1.3, $|N\rangle$ is one of the ground states of the Sn-isotopes around $N_a = 68$.

Making use of the fact that $E_R = (\hbar^2/2J)(N-N_0)^2$ and that $\delta N \ll 1$, the wavepacket (3.7.21) will decay into one of the states $|N\rangle$, likely the one corresponding to $N = \sum_{\nu>0} 2V_\nu^2$, in a time \hbar/E_R . The number of Cooper pairs participating in the nuclear condensate is

in the case of ^{120}Sn is $\approx 5-6$, the number of neutrons thus being $206 \approx 10$. Because $\delta N \sim \sqrt{N} \sim 3$ ($\delta\phi \sim 0.3 \text{ rad}$, that is $\delta\phi \sim 0.3/0.017 \approx 17^\circ$), one obtains $E_R \approx 0.092 \text{ MeV} \cdot (3)^2 \approx 1 \text{ MeV}$ ($\hbar^2/2J \approx \hbar^2/4 \approx 25 \text{ MeV}/(4N_0)$) $\approx 0.092 \text{ MeV}$, see Fig. 2.1.3). Consequently $\hbar/E_R \approx 10^{-21} \text{ s}$.

Further insight into the same question can be obtained making use of (3.7.10). That is $1/\dot{\phi} \approx \hbar/E_F \approx \hbar/(36 \text{ MeV}) \approx 3 \times 10^{-23} \text{ s}$. In other words, superfluid nuclei prepared in isolation, in a state displaying a coherent superposition of N -values, will decay into a member of the corresponding pairing rotational band of which (3.7.19) (see also (3.7.21)) is the intrinsic state, becoming stabilized on the particular state $|N\rangle$ after about 30 revolutions. The common assumption that N is fixed and $\dot{\phi}$, ^{not} meaningless, is correct.

This is also the case for metallic superconductors. In fact, the state (3.7.17) even if prepared in rotation will disintegrate because there is a term in the energy of the superconductor depending on N , namely the electrostatic energy $e^2(N-N_0)^2/2C$, where C is the electrostatic capacity. Because the number of overlapping Cooper pairs contributing to superconductivity is $\approx 10^6$ and thus the associated

**) The capacity of a sphere is $C = R$. Below we use $R = 1 \text{ cm}$.

*) $\delta\phi \approx 0.3/(\pi/180) \approx 0.3/0.017 \approx 17^\circ$.

number of electrons $2\alpha'_0 \approx 2 \times 10^6$, $\delta N \approx \sqrt{N} \approx 10^3$, (256)
one can write $E_{el} = \frac{e^2}{2c} (\delta N)^2 \approx \frac{14.4 \text{ eV} \times 10^{-8} \text{ cm}}{2 \times 1 \text{ cm}^2} (10)^3 \approx 10^7 \text{ MeV}$,

and $\tau/E_{el} \approx 10^{-14} \text{ s}$. Similarly as done in connection with atomic nuclei, we estimate $(\dot{\phi})^{-1} = \tau/(4 \text{ eV}) \approx 10^{-16} \text{ s}$, implying in this case about 10^2 revolution to loose the original N -wavepacket coherence. In this case $\delta\phi \approx 10^{-3}$ radians, that is $\delta\phi \approx 10^{-3}/0.017 \approx 1^\circ$.

(to p. 256)

8